Pergamon

Pattern Recognition, Vol. 30, No. 10, pp. 1661–1671, 1997

0031-3203/97 $17.00+.00

PII: S0031-3203(96)00183-5

A CURVE BEND FUNCTION BASED METHOD TO CHARACTERIZE CONTOUR SHAPES

ALAN M. N. FU*, HONG YAN and KAI HUANG
Department of Electrical Engineering, University of Sydney, NSW 2006, Australia

(*Received* 5 *October* 1995; *in revised form* 7 *November* 1996)

Abstract—In this paper, a new Curve Bend Function (CBF) based method is presented to extract main features of a contour. It utilizes two quantities, one called a Curve Bend Angle (CBA), and the other known as a type coefficient of curve segment defined on a contour. The CBA measures the bending degree at each point on the contour, while the type coefficient characterizes the properties (convexity and concavity) of simple curve segments. The CBF combines the advantages of the two quantities and provides an overall description of a contour. A local maximum or minimum of the CBF corresponds to a critical point of the contour, and the peak value is the cosine of the CBA. Hence, the problem of locating critical points of a contour is reduced to the problem of finding peak points of the CBF. The sign of a peak value indicates the related CBA being an inner or outer angle. Our experimental results and comparisons between the CBF method and Rosenfeld–Johnston's method show that our method is effective and accurate in generating the description of a contour. © 1997 Pattern Recognition Society. Published by Elsevier Science Ltd.

Simple curve Compound simple curve Curve bend angle Curve bend function

1. INTRODUCTION

Contour feature representation is a crucial issue in pattern recognition and computer vision applications. In general, a contour can be comprised of several elements including line segments and arcs (convex or concave curve segments). The joining points between the elements are called critical points. A critical point may be a vertex of an angle, or an intersection of a line segment and an arc, or an intersection of two arcs. A critical point of a contour which is not a vertex of an angle is known as a corner. Thus features of a contour comprise critical points, line segments, arcs and their properties (convexity or concavity). The key step in feature representation of a contour is to find the set of critical points.

Many methods have been developed in the past for contour description.[1–17] These methods can be classified into three classes. The first class includes methods which search for dominant (critical) points using some significance measure other than curvature. For example, Rosenberg's method[1,2] belongs to this class. The method was developed to extract fragments of a convex blob which are perceptually meaningful. This was achieved by attributing to each point of the blob a set of neighboring points and finding the significant set. A corner is determined by the significant set. This method can be used to find the location of an angle, but it cannot determine the magnitude of the angle.

The second class includes methods in which the curvature is evaluated after transforming the contour to the Gaussian scale space.[14–16] One advantage of this class of methods is that they are suitable for extracting features from a noisy curve. However, a long computing time is needed to construct the Gaussian scale space. Another disadvantage of the method is that it cannot estimate the magnitude of an angle.

The third class comprises methods in which a curvature is employed directly to search for critical points in the original picture space.[3–12] The methods are effective to locate critical points on a contour if the related parameters are selected suitably. Some methods can only locate critical points on a contour,[7] while some others can not only determine the position of an angle, but also evaluate the magnitude of the angle.[4–6] Rosenfeld's algorithm has one parameter, the supported length [or the smoothing factor[6]], which needs to be assigned initially. The accuracy in estimating the size of an angle by this method depends on the supported length. This method may produce redundant points or miss some critical points[6,13] when the supported length used is not suitable. Also, the method is not able to identify directly whether an angle on a contour is an inner or outer one. This is because it cannot distinguish angles α and $360°-\alpha$ of the contour if both angles exist. Davis[13] proposed two algorithms, ADS (angle detector—sequential) and ADP (angle detector—parallel), for searching the supported length (region). In these algorithms there are two unknown parameters related to the supported region which need to be assigned initially. Teh and Chin proposed an algorithm[6] which requires no input parameter to detect critical points on digital curves. However, the technique is not always effective. This is discussed in more details below. Let C be a contour (closed curve),

$$C = \{S_i = (x_i, y_i),\ i = 0, \ldots, N-1\}, \qquad (1)$$

where (x_i, y_i) is an integer-coordinate of the point S_i on

* Author to whom correspondence should be addressed. Tel.: +61 2 351-4824; fax: +61 2 351-3847; e-mail: alanf@ee.usyd.edu.au.

the contour, and S_{i+1} is a neighbor of S_i. For convenience, C is considered being a periodic sequence with the period N, i.e. we have $S_i = S_{N-i}$, $i = 0, \ldots, N-1$. Let e_{ik} and d_{ik} denote the distance between points S_{i-k} and S_{i+k} and the distance from point S_i to chord $S_{i-k}S_{i+k}$, respectively. Teh and Chin's algorithm is presented as follows:

Start with $k = 1$. Compute e_{ik} and d_{ik} until

$$e_{ik} \geq e_{ik+1} \tag{2}$$

or

$$\frac{d_{ik}}{e_{ik}} \geq \frac{d_{ik+1}}{e_{ik+1}} \quad \text{for } d_{ik} > 0, \tag{3}$$

$$\frac{d_{ik}}{e_{ik}} \leq \frac{d_{ik+1}}{e_{ik+1}} \quad \text{for } d_{ik} < 0. \tag{4}$$

Let $D(S_i)$ denote the set of points which satisfy either equation (2) or equations (3) and (4), i.e.

$$D(S_i) = \{(S_{i-k}, \ldots, S_{i-1}, S_i, \ldots, S_{i+k}) \mid \text{equation (2) or equations (3) and (4)}\}, \tag{5}$$

then $D(S_i)$ is the support region of S_i.

However, the above technique does not work in some cases. For example, the contour shown in Fig. 1 satisfies the following conditions:

(i) Angle $\angle S_{i-L}S_iS_{i+L}$ is larger than 60°.

(ii)

$$e_{ij+1} = e_{ij} + 1, \quad j = L, L+1, \ldots, M, \tag{6}$$

(iii)

$$d_{ij+1} = d_{ij} + 1, \quad j = L, L+1, \ldots, M, \tag{7}$$

where S_{i-L} is the vertex of angle $\angle S_iS_{i-L}S_{i-M}$. It is obvious that condition in equation (2) is not satisfied when $k < M$. We can also show that equations (3) and (4) are not satisfied either when $k < M$. Based on condition (i), we have $(d_{iL}/e_{iL}) < 1$, i.e.

$$d_{iL} < e_{iL}. \tag{8}$$

If equation (3) is satisfied, substituting equations (6) and (7) into equation (3) we have

$$\frac{d_{iL}}{e_{iL}} \geq \frac{d_{iL}+1}{e_{iL}+1},$$

and therefore

$$e_{iL} \leq d_{iL}, \tag{9}$$

which is in contradiction with equation (8). Thus, equation (3) must not be satisfied when $k < M$. Similarly, it can be shown that equation (4) is not satisfied either when $k < M$. Thus, the performance for searching the supported region of point S_i by the algorithm does not stop when $k = L$. Hence the region of support of S_i obtained by the technique is incorrect in this case. The determination of region of support is a quite difficult task, and an algorithm which is really effective for solving the problem has not been found so far.

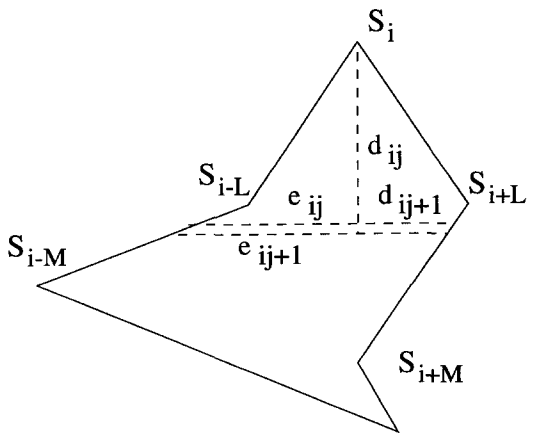

Fig. 1. Contour for verifying Teh and Chin's algorithm.

The existing techniques were mainly developed to search for critical (dominant) points on a contour. As mentioned above, some of them do not only find the location of a corner but also have the ability to evaluate the magnitude of an angle, if the angle exists. It is well known that information which includes only critical points and sizes of angles of a contour is not enough to determine the contour in general.

In the view of human perception, a complete description of a contour should comprise the following four aspects:

1. Critical point where the contour has a local maximum significant measure (curvature or an alternative quantity which is proportional to the curvature, such as the chord height).
2. Magnitude of an angle.
3. Property of an angle (i.e. inner or outer).
4. Property of edges of an angle (convex or concave).

In this paper, a new method based on the combination of a quantity called *curve bend angle* and a quantity known as *type coefficient of a curve segment* is presented to generate a description for a contour, which solves the first three problems and partly solves the last problem. The information obtained by the proposed method includes key features of the contour.

The remainder of the paper is organized as follows: in Section 2, the Curve Bending Function (CBF) and its properties are introduced. In Section 3, the procedures based on CBF for generating the description of a contour are presented. Our experimental results and conclusions are given in Sections 4 and 5, respectively.

2. CURVE BENDING FUNCTION AND ITS PROPERTIES

The contour of an object is a continuous closed planar curve defined on R^2. To analyze the properties of a contour numerically, a contour considered in this paper is assumed to be the boundary of an object represented by the binary image:

$$I(x,y) = \begin{cases} 1 & \text{if } (x,y) \in \text{object}, \\ 0 & \text{otherwise.} \end{cases} \tag{10}$$

The points on a contour can be traced and labeled anticlockwise from an arbitrary starting point, and therefore the contour can be represented by the array: $\Omega = \{S_k,\ k = 0, 1, \ldots, N-1\}$, where N is the total number of points of the contour. Without loss of the generality, suppose S_0 and S_{N-1} are the starting and ending points of the contour, respectively. Since a contour is a closed curve, we can consider that $S_{N+i} = S_i$ and $S_{-i} = S_{N-i}$, $i = 0, \ldots, N-1$, i.e. the contour Ω is treated as a periodic sequence with the period N.

In order to investigate the features of a contour, we first derive two geometric theorems concerning a closed planar curve, and then present a scheme for searching the main features of a contour based on these theorems.

Suppose $J = \alpha N$ is a positive integer, called the supported length, where $0 < \alpha < 1$ is referred to as the supported rate. Let $\Omega_i(J)$ denote the portion of Ω:

$$\Omega_i(J) = \{S_{i-J}, \ldots, S_i, \ldots, S_{i+J}\}, \tag{11}$$

and it is called J-neighborhood (J-nb) of point S_i.

Let

$$h_i^J(k) = \rho(S_k, C_k), \quad S_k \in \Omega_i(J), \tag{12}$$

where $i - J < k < i + J$, $\rho(S_k, C_k)$ denotes the distance between S_k and C_k, C_k lies on line segment $S_{i-J}S_{i+J}$ and S_kC_k is perpendicular to $S_{i-J}S_{i+J}$.

Definition 1. The point $S_k \in \Omega_i(J)$ is known as a local maximum point of Ω, if there is $0 < K \le K_0$ such that $h_i^J(k) > h_i^J(k \pm j)$, $j = 1, \ldots, K$, where $K_0 = \mathrm{Min}\{k - i + J, i + J - k\}$.

Definition 2. $\Omega_i(J)$ is known as a simple curve if $\Omega_i(J)$ does not contain more than one local maximum point of Ω. If all $\Omega_i(J)$, $i = 0, 1, \ldots, N-1$, are simple curves, then Ω is known as a Compound Simple Curve (CSC) with step length J denoted by $\Omega(J)$.

The curves shown in Fig. 2(a)–(c) are simple curves, while Fig. 2(d) and (e) are not. Obviously, if $\Omega(J)$ is a CSC, then so is $\Omega(J')$, where $0 < J' < J$. For a given J, if each J-nb, $\Omega_i(J)$, is a simple curve, then the J is recognized to be the suitable supported length. It is clear that J' is suitable if J is suitable where $0 < J' < J$.

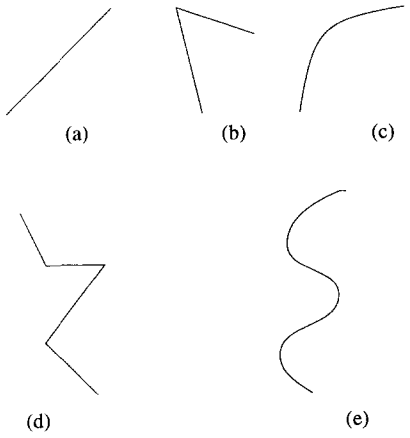

Fig. 2. Five types of curve segments.

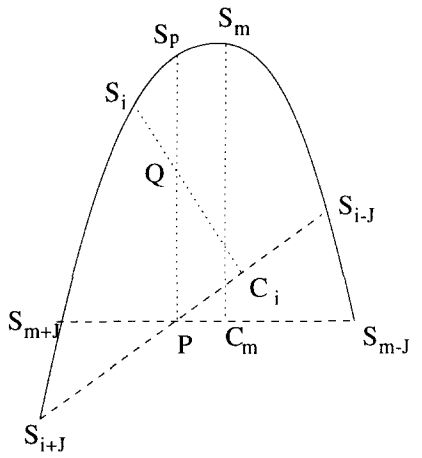

Fig. 3. The explanation of the proof of Lemma 1.

Lemma 1. Suppose that the contour $\Omega(J)$ is a CSC. If S_m is a local maximum point, then

$$h_m^J(m) > h_i^J(i),$$
$$i = m - J, \ldots, m-1, m+1, \ldots, m+J. \tag{13}$$

Proof. Suppose $m < i < m + J$, and P is an intersection of $S_{m-J}S_{m+J}$ and $S_{i-J}S_{i+J}$ (Fig. 3). Through point P we draw a perpendicular line of $S_{m-J}S_{m+J}$, which meets line S_iC_i and $\Omega_i(J)$ at Q and S_p, respectively. Since $\Omega_m(J)$ is a simple curve and S_m is a local maximum point, we have $h_m^J(m) > PS_p$. On the other hand, since $S_iC_iS_{i-J}S_{i+J}$, $h_i^J(i) = \rho(S_i, C_i)$ and $\angle PC_iQ = 90°$, we have $QP > QC_i$ and $QS_p > QS_i$. Therefore, $PS_p > S_iC_i$, i.e. $PS_p > h_i^J(i)$. By combining above results, we obtain $h_m^J(m) > h_i^J(i)$, $m < i < m + J$. Similarly, we can show that equation (13) is held for $m - J < i < m$. Hence, the lemma is proved.

Lemma 2. Suppose $\Omega(J)$ is a CSC. If S_m is a local maximum point, then

$$\beta_m^J < \beta_i^J, \quad i = m - J, \ldots, m-1, m+1, \ldots, m+J, \tag{14}$$

where $\beta_i^J = \angle S_{i-J}S_iC_i$ (see Fig. 4).

Proof. Let S_m and S_mC_m coincide with S_i, and S_iC_i, respectively (Fig. 4). Since $\Omega(J)$ is a CSC, $\Omega_m(J) = \{S_{m-J}, \ldots, S_m, \ldots, S_{m+J}\}$ is a simple curve. Since S_m is a local maximum point, based on Lemma 1, we have

$$h_m^J(m) > h_i^J(i),$$
$$i = m - J, \ldots, m-1, m+1, \ldots, m+J, \tag{15}$$

i.e. $\rho(S_i, C_i) < \rho(S_m, C_m)$. Note that $\tilde{\rho}(\widetilde{S_{i-J}S_i}) = \tilde{\rho}(\widetilde{S_{m-J}S_m})$, where $\tilde{\rho}(\widetilde{AB})$ is the length of curve $\widetilde{AB}$, so $\rho(S_i, C_i) > \rho(S_m, C_m)$. Therefore, $\beta_m^J < \beta_i^J$, for $i = m - J, \ldots, m-1, m+1, \ldots, m+J$, thus the theorem is proved.

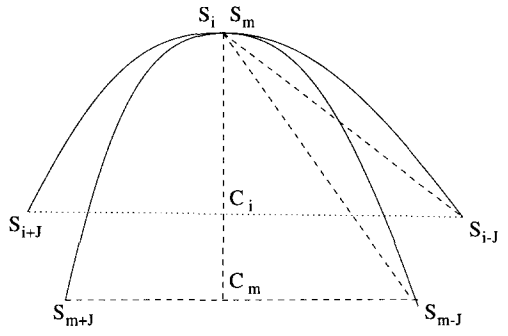

Fig. 4. The explanation of the proof of Lemma 2.

Definition 3. Suppose $\Omega(J)$ is a CSC, then a type coefficient of curve $\widetilde{S_iS_{i+2J}}$ denoted by r_i is defined as

$$r_i = 2I(O_i^x, O_i^y) - 1, \tag{16}$$

where $(O_i^x \cdot O_i^y)$ is the coordinate of the centroid of line segment $S_{i-J}S_{i+J}$.

Obviously,

$$r_i = \begin{cases} -1 & \text{if } \widetilde{S_{i-J}S_{i+J}} \text{ is concave,} \\ 1 & \text{otherwise.} \end{cases} \tag{17}$$

Definition 4. Suppose (J) is a CSC, then the *Curve Bend Function* (*CBF*) is defined as

$$\chi(S_i) = r_i \cos(\beta_i^J), \quad S_i \in \Omega(J), \tag{18}$$

where r_i is given by equation (16), $\cos(\beta_i^J) = [\rho(S_i, C_i)/\rho(S_{i-J}, S_i)]$, and $\beta_i^J = \angle S_{i-J}\widetilde{S_iC_i}$ (Fig. 4) is known as the curve bent angle of $\widetilde{S_{i-J}S_{i+J}}$ whose meaning is more general than that of "angle". A curve bent angle may be exactly half an angle on a contour, or else it is called "a corner." This is where a line segment and an arc meet or two arcs meet. In Fig. 5(a), $\angle S_{i-J}S_iS_{i+J}$ is an angle and half of its measure is the magnitude of the curve bent angle β_i^J, while in each diagram of Fig. 5(b)–(f), $S_{i-J}S_iS_{i+J}$ is not an angle, it is a corner. It can be proved that the value of CBF at a vertex is independent of J in case (a) when J is smaller than a certain critical value. However, the situation is changed for cases (b)–(f). We can further show that CBF decreases in cases (b) and (c) when J decreases, but it increases in cases (d) and (e). The relationship between $|\chi(S_i)|$ and J is very complex in the case (f) where $|\chi(S_i)|$ may increase or decrease as J decreases. These properties are held approximately for a digital curve. Based on these properties we can identify whether a curve bend angle is an angle or not.

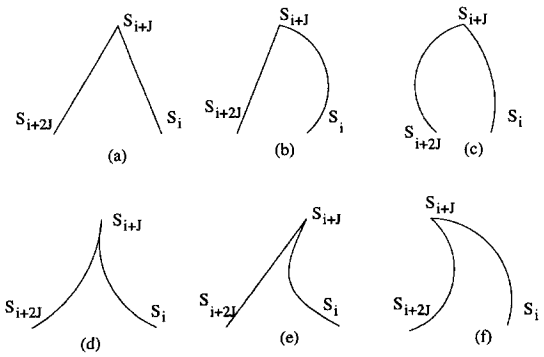

Fig. 5. Six types of corners.

Some important properties of the CBF are described below. These properties will be used to find critical points and characterize the properties of both the critical points and their J-nbs.

Theorem 1. Suppose that supported rate is selected such that $\Omega(J)$ is a CSC, and $\chi(S_i)$ is a CBF given by equation (18), then

(1)

$$\chi(S_i) \begin{cases} > 0 & \text{if } \widetilde{S_{i-J}S_{i+J}} \text{ is convex,} \\ < 0 & \text{if } \widetilde{S_{i-J}S_{i+J}} \text{ is concave,} \\ = 0 & \text{if } \widetilde{S_{i-J}S_{i+J}} \text{ is line segment.} \end{cases} \tag{19}$$

(2) $\chi(S_i)$ is a periodic function defined on $\Omega(J)$ with the period N, i.e.

$$\chi(S_{i+N}) = \chi(S_i), \quad S_i \in \Omega(J). \tag{20}$$

Proof. Using equation (17) and recalling that

$$\cos\beta_i^J = 0 \quad \text{if } \widetilde{S_{i-J}S_{i+J}} \text{ is a line segment,} \tag{21}$$

we obtain the item (1) of Theorem 1. Since $S_{i+N} = S_i$, the conclusion (2) is obvious. Note that item (2) of the theorem means that $\chi(S_i)$ is independent of the starting point of $\Omega(J)$. In other words, quantities evaluated by $\chi(S_i)$, such as the magnitude of an angle and its properties, are invariant theoretically under a rotation of a contour. However, since the coordinates of S_i are integers, the contour $\Omega(J)$ after rotating does not have the exact same shape as that of the original one, and therefore $\chi(S_i)$ has little changed when the contour is rotated. For the same reason there is a small effect on $\chi(S_i)$ when the scale of a contour is varied.

Suppose S_i is a local maximum point from equation (19), and noting the definition of J-nb then

1. if $\chi(S_i) > 0$, the J-nb of S_i is a convex curve segment;
2. if $\chi(S_i) < 0$, the J-nb of S_i is a concave curve segment;
3. if $\chi(S_i) = 0$, the J-nb of S_i is a line segment.

The value of $|\chi(S_i)|$ measures the bent degree of the J-nb of S_i, i.e. $\Omega_i(J)$. The larger $|\chi(S_i)|$, the larger bending of the $\Omega_i(J)$.

Definition 5. A local maximum point of $\Omega(J)$ is known as a critical point.

Theorem 2. S_m is a critical point of $\Omega(J)$ then

$$|\chi(S_m)| > |\chi(S_{m\pm i})|, \quad \text{for } i = 1, \ldots, J-1. \tag{22}$$

This is a direct result of Lemma 2, if we notice that $\cos(\beta^J)$, $\beta^J \in [0, \pi/2]$, is a decreasing function.

Suppose that contour $\Omega(J)$ has K critical points denoted by S_{i_k}, $k = 1, \ldots, K$, where $0 \le i_1 < i_2 < \cdots < i_K \le N-1$. For each critical point S_{i_k} we define a two-dimensional vector $\mathbf{E}_{i_k} = (\alpha_{i_k}, r_{i_k})$, $k = 1, \ldots, K$, where $\alpha_{i_k} = 2\beta^J_{i_k}$, $\beta^J_{i_k} = \cos^{-1}(|\chi(S_{i_k})|)$ [see equation (18)], and r_{i_k} is given by equation (16). The first component of $\mathbf{E}_{i_k}$, α_{i_k}, measures the bending degree of $\Omega_{i_k}(J)$. The second component, r_{i_k}, indicates that $\Omega_{i_k}(J)$ is convex or concave curve segment depending on whether r_{i_k} is equal to 1 or -1. For a given J, the K-dimensional vectors $\mathbf{G}(J,K) = \{\mathbf{E}_{i_1} \cdots \mathbf{E}_{i_K}\}$ is called the contour-vector. Thus, a contour is completely described by its contour-vector $\mathbf{G}(J,K)$, and this is confirmed by experiments presented in Section 4. In other words, geometrically, the contour is approximated by the curve-polygon with the K critical points as its vertexes. In a curve-polygon, one or both edges of a corner may be curve segments instead of straight lines. The curve-polygon is different from the existing polygonal approximation[18–20] in which the related polygons are ordinary ones so that there is no contribution of the edge information. Besides, the efficiency and accuracy of polynomial spline algorithms[20] depend on the initial location of vertexes.

3. SHAPE DESCRIPTION BASED ON CBF

Based on the results in Section 2, for an object $I(x,y)$ whose contour is represented by an array $\Omega = \{S_i = (x_i, y_i),\ i = 0, \ldots, N-1\}$, we can obtain its desciption, $\chi(S_i)$, $S_i \in \Omega$, through the following procedures:

1. Select supported rate α and get step length $J{=}\alpha N$ (in general, α ranges from 0.01 to 0.05).
2. Extend the domain of the contour:

$$S_{N+i} = S_i, \quad i = 0, 1, \ldots, N-1 \tag{23}$$

and

$$S_{-i} = S_{N-i}, \quad i = 0, 1, \ldots, N-1. \tag{24}$$

3. Determine $\chi(S_i)$ by carrying out the following two steps:
   (a) Compute r_i based on equation (16).
   (b) Compute $\chi(S_i)$ based on equation (18):

$$\chi(S_i) = \frac{r_i \rho(S_i, C_i)}{\rho(S_{i-J}, S_i)}. \tag{25}$$

4. Determine critical points based on $\chi(S_i)$. Point $S_i \in \Omega$ is considered to be a critical point if there is an $L > 0$ such that

$$|\chi(S_i)| \ge |\chi(S_{i\pm l})|, \quad l = 1, \ldots, L/2, \tag{26}$$

and

$$|\chi(S_i)| > |\chi(S_{i\pm l})| > \theta, \quad l = L/2+1, \ldots, L, \tag{27}$$

where θ is a threshold of angle, which is used to remove nearby straight angles, since a nearby straight angle is very sensitive to noise. The parameter L is selected to be larger than 20. In our experiment $\theta = 0.2$ and $L{=}20$. Due to the error of calculation, it is possible that there are two or more than two equal maximum values of $|\chi(S_i)|$ around a corner, so the relation operator "$\ge$" is used in equation (26).

5. Suppress redundant points. Due to equation (26), it is possible that there are some redundant points found as critical points obtained at Step (4). The reason for this is that there may be more than one critical point in a curve segment whose length is $2L+1$, such as in $\Omega_i(L) = \{S_{i-L}, \ldots, S_i, \ldots, S_{i+L}\}$. So all critical points of $\Omega_i(L)$ except the one in the middle location must be suppressed. After the above procedures a set of critical points of $\Omega(J)$ can be obtained and we denote them as $S_{i_1}, \ldots, S_{i_K}$.
6. Calculate magnitude of an angle based on the CBF equation (18). If S_{i_k} is a vertex, then the size of the angle is $2\beta^J_{i_k}$, where

$$\beta^J_{i_k} = \cos^{-1}(|\chi(S_{i_k})|). \tag{28}$$

If $\chi(S_{i_k}) > 0$, the angle is an inner one. If $\chi(S_{i_k}) = 0$ it is a straight angle, and it is a outer one if $\chi(S_{i_k}) < 0$.
7. Identify the nb(J) of critical point S_{i_k} [i.e. $\Omega_{i_k}(J)$] and determine whether it is a convex or concave curve segment based on $r_{i_k} = 1$ or -1.

4. EXPERIMENTAL RESULTS

To verify the effectiveness and accuracy of the CBF method, experiments on three types of contours are carried out. The first type includes three characters "F" (Fig. 6). The second type also includes three contours which are composed of both line segments and curve segments (Fig. 7). The third type includes three

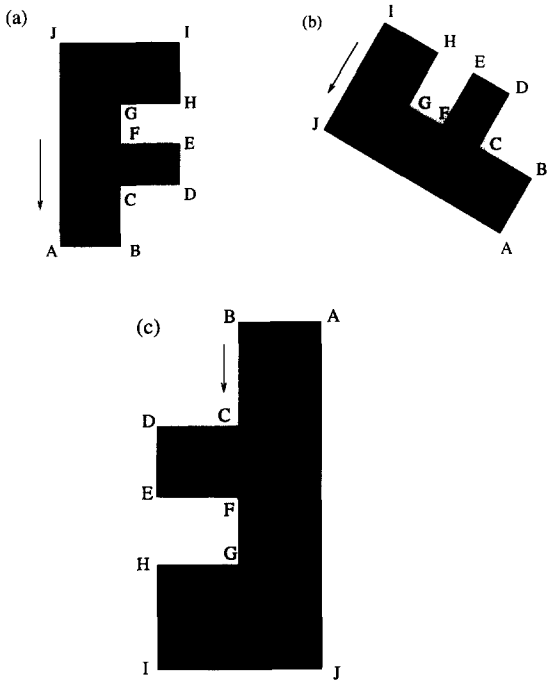

Fig. 6. Contours used for experiments.

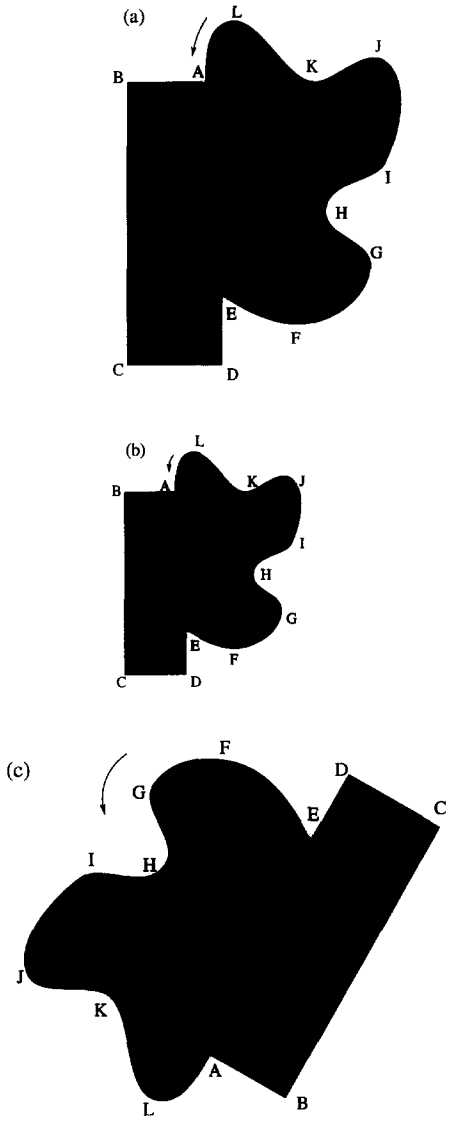

Fig. 7. Contours used for experiments.

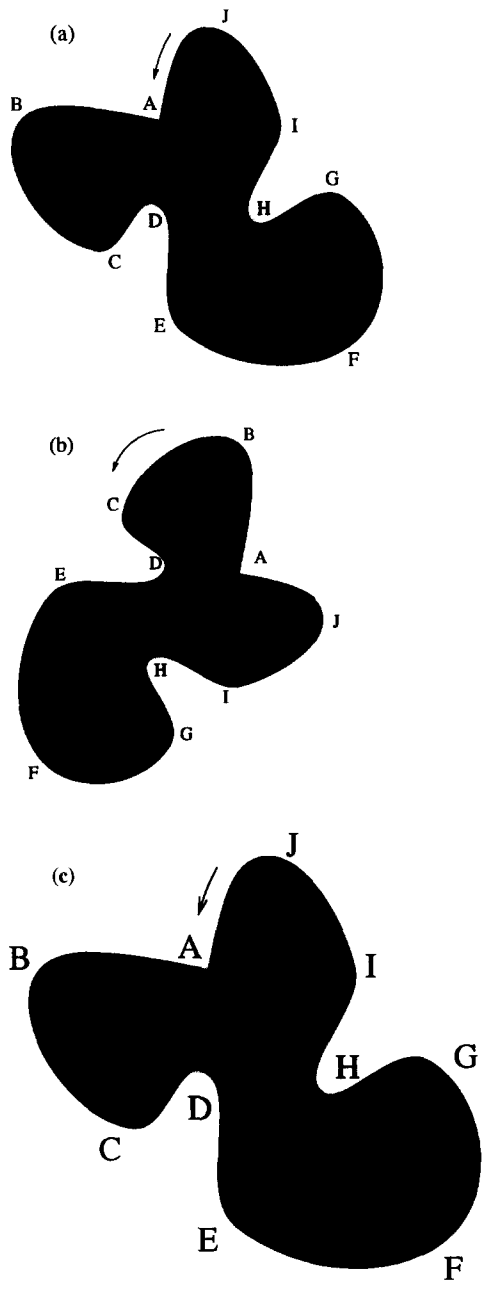

Fig. 8. Contours used for experiments.

general contours (Fig. 8). In each type, three contours have the same shape but are different in scale, or orientation, or both.

Experiments on each type of contour are performed with three different supported rates, α equals 0.02, 0.04 and 0.05 (i.e. the supported length J equals $0.02N$, $0.04N$ and $0.05N$). The experimental results shown in Fig. 9 demonstrate that the corners on the contours exactly correspond to the peaks of the graph of CBF in each case. The results also indicate clearly the properties of angles (or corners) and the properties of J-nb of each vertex, which are in agreement with the real shapes of the contours.

The experiment on the first type of contour aims to demonstrate the efficiency and accuracy of the CBF method in finding angles of a contour, estimating their sizes, and characterizing their properties (i.e. inner or outer angles) and their J-nb properties (i.e. convexity or concavity). Because the true values of angles on contours in this type are exactly known, it is possible to make a comparison between the results obtained using the CBF and Rosenfeld–Johnston's[4] methods. The results of experiments on first type of contour (Fig. 6) from our method are shown in Fig. 10 and Tables 1–3, and those obtained by Rosenfeld–Johnston's method are shown in Tables 1,2 and 3. The items with negative values in Tables 1,2 and 3 correspond to outer angles. The results show that our method is effective and accurate for both locating the position and evaluating the magnitude of an angle. The results are in agreement with those obtained by Rosenfeld–Johnston's scheme. However, our method also provides information about an angle's property (inner or outer one) and the J-nb property (convexity

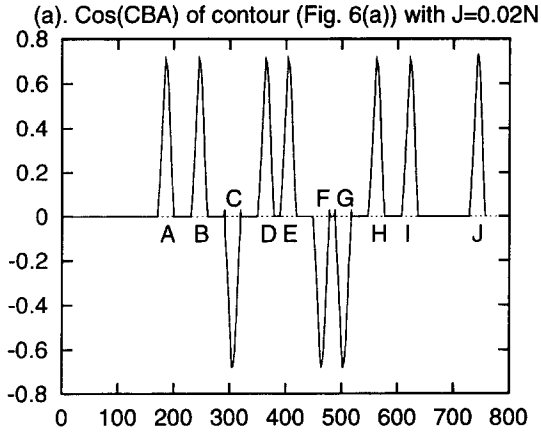

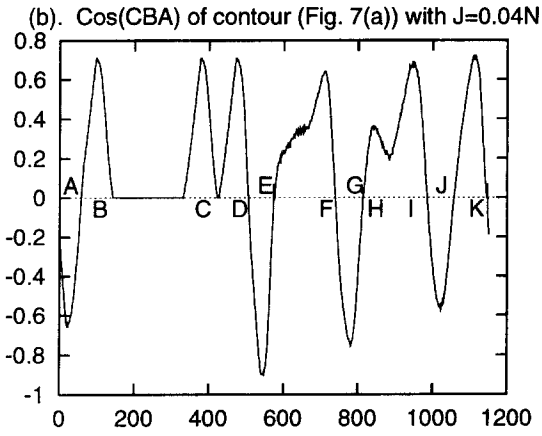

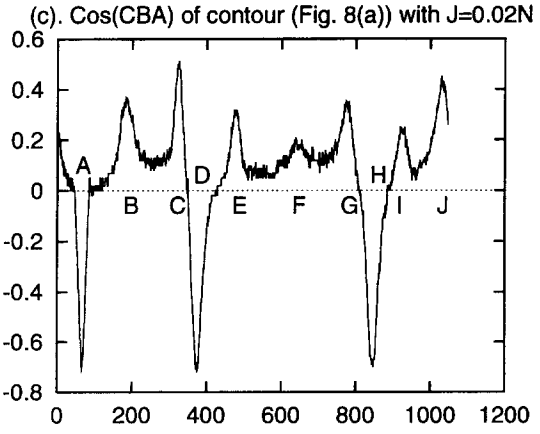

Fig. 9. The CBF of the contours in Fig. 6(a), Fig. 7(a) and Fig. 8(a).

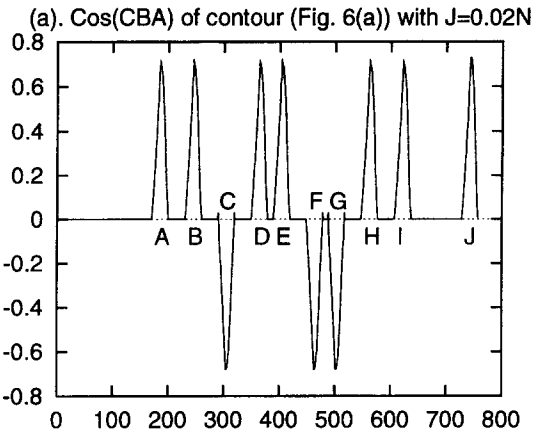

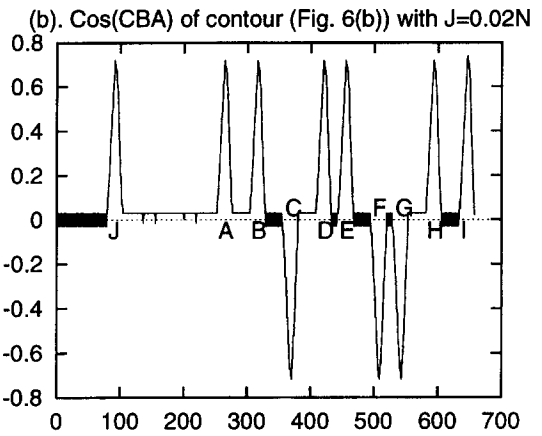

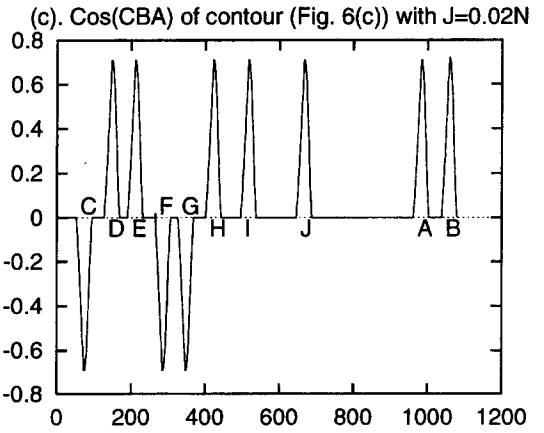

Fig. 10. The CBF of the contours in Fig. 6(a)–(c).

and concavity), which cannot be obtained by Rosenfeld–Johnston's method directly. The results also confirm that the description for a contour obtained by the CBF is invariant under scaling and rotation, which is in agreement with the theoretical analysis (see Theorem 1).

The experiments on the other two types of contours provide significant results to demonstrate the effectiveness of the CBF method. The notation "X" in Table 4 means that the angle does not exist in this case. The results in Tables 4 and 5 confirm the previous conclusions from the first type of contour. We can see that all the true right angles $\angle B$, $\angle C$ and $\angle D$ on the contours (Fig. 7) which have different scale or orientation are estimated accurately. The results are also correct in indicating the

Table 1. The angles of the contour in Fig. 6(a)

Actual sizes	CBF method			Rosenfeld–Johnston method		
	J=0.02N	J=0.04N	J=0.05N	J=0.02N	J=0.04N	J=0.05N
∠A=90°	90°	90°	90°	90°	90°	90°
∠B=90°	90°	90°	90°	90°	90°	90°
∠C=−90°	−93.7°	−91.88°	−91.53°	93.81°	91.91°	91.55°
∠D=90°	90°	90°	90°	90°	90°	90°
∠E=90°	90°	90°	90°	90°	90°	90°
∠F=−90°	−93.7°	−91.88°	−91.53°	93.81°	91.91°	91.55°
∠G=−90°	−93.7°	−91.88°	−91.53°	93.81°	91.91°	91.55°
∠H=90°	90°	90°	90°	90°	90°	90°
∠I=90°	90°	90°	90°	90°	90°	90°
∠J=90°	86.05°	88.06°	88.43°	90°	90°	90°

Table 2. The angles of the contour in Fig. 6(b)

Actual sizes	CBF method			Rosenfeld–Johnston method		
	J=0.02N	J=0.04N	J=0.05N	J=0.02N	J=0.04N	J=0.05N
∠A=90°	88.71°	90°	90°	86.69°	90°	90°
∠B=90°	88.71°	90°	90°	86.69°	90°	90°
∠C=−90°	−88.2°	−88.77°	−88.65°	93.31°	90°	90°
∠D=90°	88.71°	90°	90°	86.69°	90°	90°
∠E=90°	90°	90°	90°	90°	90°	90°
∠F=−90°	−88.2°	−88.77°	−87.86°	90°	90°	88.66°
∠G=−90°	−88.2°	−90°	−90.47°	93.31°	90°	91.34°
∠H=90°	88.71°	90°	90°	86.69°	90°	90°
∠I=90°	84.44°	88.1°	87.83°	88.04°	90°	89.22°
∠J=90°	90°	90°	90°	90°	90°	90°

Table 3. The angles of the contour in Fig. 6(c)

Actual sizes	CBF method			Rosenfeld–Johnston method		
	J=0.02N	J=0.04N	J=0.05N	J=0.02N	J=0.04N	J=0.05N
∠A=90°	90°	90°	90°	90°	90°	90°
∠B=90°	87.21°	88.65°	88.93°	90°	90°	90°
∠C=−90°	−92.66°	−91.32°	−91.05°	92.73°	91.33°	91.06°
∠D=90°	90°	90°	90°	90°	90°	90°
∠E=90°	90°	90°	90°	90°	90°	90°
∠F=−90°	−92.66°	−91.32°	−91.05°	92.37°	91.33°	91.06°
∠G=−90°	−92.66°	−91.32°	−91.05°	92.37°	91.33°	91.06°
∠H=90°	90°	90°	90°	90°	90°	90°
∠I=90°	90°	90°	90°	90°	90°	90°
∠J=90°	90°	90°	90°	90°	90°	90°

properties of both angles (or corners) and their J-nbs (see Table 5). The measure of a corner (not angle) depends on J. Although the real measure for a corner is not available, for a given J, the measure of a corner by the CBF is still significant, because it is approximately invariant under scaling and rotation (see Table 4). As mentioned in Section 2, due to the fact that a contour is represented by finite points, i.e. S_i, $i = 0, \ldots, N-1$, and the coordinates of each point are integers, the shape of the contour does not remain completely the same as the original after a rotation or change in its scaling. The results in Table 4 show the effect of the rotation and scaling on CBF. We find that recovered angles have little error (less than 3°) given scale change, and relatively much more for orientation change. This is because the CBF (see Definition 4) is associated with a cosine function which describes the shape of a contour and because the effect of given scale change on the shape of the contour is less than that of given orientation change. Note that a few large corners (i.e. its measure near a straight angle) may appear or disappear under scaling and rotation (see Table 4 for the corner "F" on the contour in Fig. 7). This problem can be overcome by setting a suitable threshold to suppress larger corners.

Table 4. The effect of scale change and rotation on CBF

Actual sizes	CBF method								
	J=0.02N			J=0.04N			J=0.05N		
	Fig. 7(a)	Fig. 7(b)	Fig. 7(c)	Fig. 7(a)	Fig. 7(b)	Fig. 7(c)	Fig. 7(a)	Fig. 7(b)	Fig. 7(c)
A: corner	−94.98°	−93.47°	−91.54°	−98.92°	−98.87°	−101.35°	−104.71°	−104.78°	−105.47°
∠B=90°	90°	90°	90°	90°	90°	89.9°	90°	90°	89.91°
∠C=90°	90°	90°	90°	90°	90°	89.9°	90°	90°	90.29°
∠D=90°	90°	90°	90°	90°	90°	89.9°	90°	90°	89.68°
E: corner	−43.05°	−43.93°	−50.2°	−50.74°	−51.13°	−53.38°	−54.82°	−56.72°	−56.44°
F: corner	153.53°	153.53°	155.69°	X	X	149.81°	X	X	X
G: corner	118.74°	121.31°	131.49°	100.04°	102.87°	108.67°	96.08°	96.57°	100.19°
H: corner	−114.51°	−111.57°	−120.12°	−82.77°	−84.53°	−91.15°	−80.53°	−81.85°	−85.34°
I: corner	141.98°	143.13°	137.36°	137.25°	138.49°	128.17°	136.44°	136.92°	126.35°
J: corner	123.14°	124.48°	120.77°	93.95°	94.16°	97.70°	85.63°	85.69°	90°
K: corner	−128.14°	−130.69°	−130.32°	−111.13°	−111.58°	−117.41°	−109.45°	−108.51°	−113.85°
L: corner	114.30°	111.24°	122.03°	87.09°	88.38°	82.34°	79.92°	82.24°	72.41°

Table 5. The description of the contours in Fig. 8 with J=0.02N

Ctl. points	Fig. 9(a)		Fig. 9(b)		Fig. 9(c)	
	Size of cnr.	nb(J)	Size of cnr.	nb(J)	Size of cnr.	nb(J)
A	−90°	concave	−90°	concave	−90°	concave
B	137.1°	convex	137.1°	convex	129.21°	convex
C	118.8°	convex	118.8°	convex	115.23°	convex
D	−87.28°	concave	−87.28°	concave	−83.09°	concave
E	142.11°	convex	142.11°	convex	136.1°	convex
F	156.68°	convex	156.68°	convex	151.02°	convex
G	138.56°	convex	138.56°	convex	130.05°	convex
H	−91.86°	concave	−91.86°	concave	−79.47°	concave
I	151.52°	convex	151.52°	convex	145.42°	convex
J	125.97°	convex	127.13°	convex	112.51°	convex

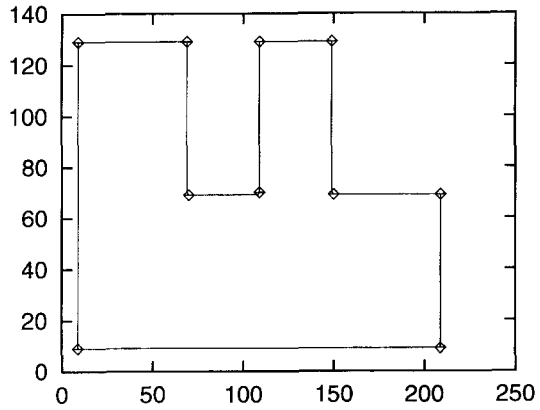

Fig. 11. The critical points of the contour in Fig. 6(a) obtained by the CBF with J=0.02N.

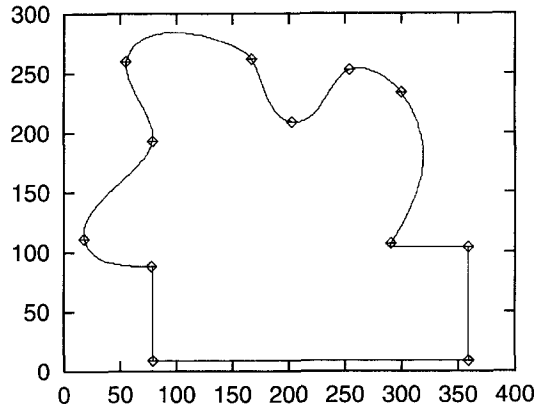

Fig. 12. The critical points of contour [Fig. 7(a)] found by the CBF with J=0.02N.

The critical points of contours [Fig. 6(a), 7(a) and 8(a)] obtained by the CBF, denoted by small "square", are shown in Fig. 11–13, respectively. It is clear that the critical points exactly coincide with the actual vertexes (or corners) of the contours which we expect to find [since the contours in Fig. 6(a), 7(a) and 8(a) are obtained from "xfig-window" by these critical points, respectively]. We can see that the contour-vector, $\mathbf{G}(J,K)$, obtained by the CBF is sufficient to describe the contour when the supported rate α is selected suitably. For Fig. 7, in the case where $J = 0.02N$, there are 12 critical points of each contour found by CBF (see Table 4) which include the 11 points that are found by CBF with J in the range $0.04N$–$0.05N$. The additional point (corner

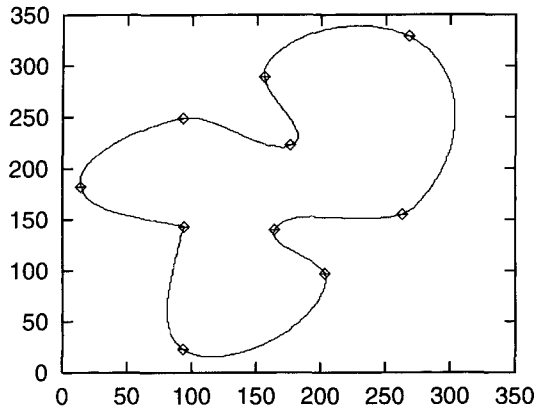

Fig. 13. The critical points of contour [Fig. 8(a)] found by the CBF with $J=0.02N$.

"F") does not affect the shape of the contour. For the contour (Fig. 8) we have the same conclusion as that of Fig. 7 discussed above.

The description of a contour obtained by CBF method has been successfully utilized in shape recognition tasks in conjunction with a neural network module.[21,22] Note that in references (21,22), the definitions of curved bend angle β_i^J are different, but they have the same effectiveness and accuracy in solving the problem of shape recognition and classification.

5. CONCLUSIONS

A CBF based method for searching critical points of a contour is presented and its effectiveness and reliability in generating the description of the contour are demonstrated. The experiment results confirm that the description obtained by the method is essentially invariant under scaling and rotation.

The essence of the CBF method in locating critical points is searching for peaks of the CBF. If the peak is a local maximum then the corresponding CBA is an inner angle and its J-nb is a convex curve segment, otherwise if the peak is a local minimum, the CBA is an outer one and its J-nb is a concave curve segment. The location of a CBA is found with high accuracy (see Figs 11,12 and 13), and its size is also estimated with small error [note that the measure of a corner (not angle) depends on J] (see Tables 1,2,3 and 4). Based on this information, the contour is approximated by a contour-vector, $\mathbf{G}(J,K)$, where K is the total number of critical points on the contour.

In the CBF method, the supported rate α (or the step length $J=\alpha N$) is assigned initially. In our experiments α ranges from 0.02 to 0.05. In practical application, α should be selected based on the nature of the contour to be analyzed. Some unexpected results may be produced if α is not used suitably. How to choose an appropriate α for a variety of contours is an important issue, and it needs further investigation.

It seems that it is a shortcoming of the CBF that the supported rate α of a contour needs to be assigned initially without sufficient information about the contour. However, it will become an advantage when the searching for critical points of a contour is made for contour recognition. This is because the value of α can be determined effectively from the model contour, and different models should have a different α in general, so it is expected that the recognition rate of contours can be improved when α is selected based on the individual model. In fact, the contour-vector generated by the CBF has been successfully applied to solve shape recognition problems.[21,22]

REFERENCES

1. B. Rosenberg, The analysis of convex blobs, *Comput. Graphics Image Process.* **1**, 183–192 (1972).
2. B. Rosenberg, Computing dominant point on simple shapes, *Int. J. Man-Machine Studies* **6**, 1–12 (1974).
3. I. M. Anderson and J. C. Bezdek, Curvature and tangential deflection of discrete arcs: A theory based on the commutator of scatter matrix pairs and its application to vertex detection in planar shape data, *IEEE Trans. Pattern Analysis Mach. Intell.* **PAMI-6**(1), 27–40 (1984).
4. A. Rosenfeld and E. Johnston, Angle detection on digital curves, *IEEE Trans. Comput.* **C-22**, 875–878 (1973).
5. A. Rosenfeld and J. S. Weszka, An improved method of angle detection on digital curves, *IEEE Trans. Comput.* **C-24**, 940–941 (1975).
6. C. H. Teh and R. T. Chin, On the detection of dominant points on digital curves, *IEEE Trans. Pattern Analysis Mach. Intell.* **11**(8), 859–872 (1989).
7. P. Zhu and P. M. Chirlian, On critical point detection of digital shapes, *IEEE Trans. Pattern Analysis Mach. Intell.* **17**(8), 737–748 (1995).
8. N. Katzir, M. Lindenbaum and M. Porat, Curve segmentation under partial occlusion, *IEEE Trans. Pattern Analysis Mach. Intell.* **16**(5), 513–519 (1994).
9. M. Katagiri and M. Nagura, Recognition of line shapes using neural networks, *IEICE Trans. Inf. Syst.* **E77-D**(7) (1994).
10. H. Freeman, On the encoding of arbitrary geometric configurations, *IER Trans. Comput.* **EC-10**, 260–268 (1961).
11. H. Freeman and L. S. Davis, A corner finding algorithm for chain code curve, *IEEE Trans. Comput.* **C-26**, 297–303 (1977).
12. Y. Lin, J. Dou and H. Wang, Contour shape description on an arch height function, *Pattern Recognition* **1**, 17–23 (1992).
13. L. S. Davis, Understanding shape: Angles and sides, *IEEE Trans. Comput.* **C-26**(3), 236–242 (1977).
14. F. Moktarian and A. K. Mackworth, A theory of multiscale-based shape representation for planar curves, *IEEE Trans. Pattern Analysis Mach. Intell.* **14**(8), 789–805 (1992).
15. A. Rattarangsi and R. T. Chin, Scale-based detection of corners of planar curves, *IEEE Trans. Pattern Analysis Mach. Intell.* **14**(4), 430–449 (1992).
16. N. Ueda and S. Suzuki, Learning visual models from shape contours using multiscale convex/concave structure matching, *IEEE Trans. Pattern Analysis Mach. Intell.* **15**(4), 337–352 (1993).
17. D. Cyganski and J. A. Orr, The tensor differential scale space representation, *NATO ASI Ser.* **F-30**, 471–479 (1987).
18. J. H. Wu and J. J. Leou, New polygonal approximation schemes for object shape representation, *Pattern Recognition* **26**(4), 471–484 (1993).

19. D. A. Mitzias and B. G. Mertzios, Shape recognition with a neural classifier based on a fast polygon approximation technique, *Pattern Recognition* **27**(5), 627–636 (1994).
20. T. Pavlidis and R. L. P. Chang, Application of fuzzy sets in curve fitting, *Proc. IEEE 1977 Decision and Control Conference*, 1396–1400 (1977).
21. Alan M. N. Fu and Hong Yan, A shape classifier based on Hopfield–Amari network, *Proc. ICNN* (June 1996).
22. Alan M. N. Fu and Hong Yan, Contour classification by a Hopfield–Amari network, *Proc. ICONIP* (September 1996).

About the Author — ALAN MINGNAN FU obtained a B.Sc. degree in 1963 from the Department of Mathematics and Mechanics, Zhongshun (Dr Sunyatsen) University, China, and become an Associate Professor (1988–1989) in the Department of Applied Mechanics and Engineering. He is currently a Research Assistant and working toward the Ph.D. degree in the Department of Electrical Engineering, University of Sydney. His research interests include neural networks, relaxation, image processing and pattern recognition.

About the Author — HONG YAN received his B.E. degree from Nanking Institute of Post and Telecommunications in 1982, M.S.E. degree from the University of Michigan in 1984, and Ph.D. degree from Yale University in 1989, all in Electrical Engineering. From 1986 to 1989 he was a Research Scientist at General Network Corporation, New Haven, CT, U.S.A., where he worked on developing a CAD system for optimizing telecommunication systems. Since 1989 he has been with the University of Sydney where he is currently a Professor in Electrical Engineering. His research interests include medical imaging, signal and image processing, computer vision, neural networks and pattern recognition. He is an author or co-author of more than 150 technical papers in these areas. Dr Yan is a senior member of the IEEE, and a member of the SPIE, the International Neural Network Society, the Pattern Recognition Society, and the Society of Magnetic Resonance.

About the Author — KAI HUANG received his B.Sc. degree in Computer Science and Pure Mathematics in 1991 and B.E.(Honours) degree in Electrical Engineering in 1993, both from the University of Sydney. He is currently a Ph.D. student in the Department of Electrical Engineering at the University of Sydney. His research interests include pattern recognition, signal and image processing and automatic handwritten signature verification.